Pressure behavior of the sound velocity of liquid water at room temperature in the terahertz regime

M. Santoro,[1,2,*] F. A. Gorelli,[1,2] T. Scopigno,[2,4] M. Krisch,[3] F. Sette,[3] and G. Ruocco[2,4]
[1]*LENS, European Laboratory for Nonlinear Spectroscopy, I-50019 Sesto Fiorentino, Firenze, Italy*
[2]*IPCF-CNR, UOS Roma "La Sapienza", I-00185 Roma, Italy*
[3]*European Synchrotron Radiation Facility, 38043 Grenoble, France*
[4]*Dipartimento di Fisica, Università di Roma "La Sapienza", I-00185 Roma, Italy*
(Received 9 June 2011; published 20 September 2011)

The pressure evolution of the sound velocity in liquid water in the terahertz regime, c_∞, between 0.05 and 0.88 GPa, at room temperature, has been investigated by synchrotron inelastic x-ray scattering in a diamond anvil cell. We confirm previous results showing that c_∞ increases with density much less than the adiabatic sound velocity c_s, which is reasonably related to the known structural modifications in the hydrogen bond network. At variance with a previous study where an anomaly was found in the density evolution of c_∞—most likely due to the nonisothermal character of the study—the present work reveals a smooth behavior of c_∞, which could provide a useful constraint to the current theories on liquid water.

DOI: 10.1103/PhysRevB.84.092301 PACS number(s): 78.70.Ck, 62.50.−p, 62.60.+v

The pressure and temperature evolution of the dynamical and structural properties of liquid water has led to the production of a vast scientific literature in the last few decades. Remarkably, some of the most relevant aspects are still unsolved. Experimental and computational studies of the structure in the 0–6.5 GPa and 240–670 K pressure-temperature (P-T) range show a general consensus in at least three facts: (i) Liquid water is most likely to be made of the coexistence of two different states, low-density water (LDW) and high-density water (HDW); (ii) the weight of the HDW (LDW) state in the overall structure of water increases (decreases) upon increasing pressure, and the evolution is continuous; (iii) the difference between the two forms is mainly related to changes in the structure of the second coordination shell of the molecules, while the first one remains substantially unaltered with H_2O in tetrahedral coordination by the nearest-neighbor molecules through the hydrogen bond.[1–4] Though different scenarios are evoked for the densification mechanism, they all reveal that the effective number of nearest-neighbor molecules in liquid water continuously increases upon increasing pressure [up to 12 at 4.5 GPa and 500 K (Ref. 4)], due to the shift of interstitial non-hydrogen-bonded molecules that tend to enter the first coordination shell from the second one.[2] Interestingly, although the central pentamer hardly changes with pressure, the overall high-pressure structure develops characteristic simple liquid features as shown by the oxygen-oxygen pair distribution function.[3] The pressure dependence of the properties of liquid water is nowadays rationalized by different theoretical models, which extend to low temperatures in the deeply supercooled regime, not accessible by experiments.[5] One of these models predicts a true, first-order phase separation between LDW and HDW in the supercooled region, along a *P-T* coexistence line which ends in a secondary critical point located at 0.18–0.32 GPa, and ∼220–250 K.[6] Recent dynamical studies of the isothermal pressure behavior of the adiabatic sound velocity and of the O-H stretching frequencies at 0–6 GPa and 293–573 K, based on Brillouin[7] and Raman[8] spectroscopy, respectively, have shown very small anomalies (cusps). The loci of these cusps in the *P-T* plane form two lines, one for the Brillouin and one for the Raman study, respectively, which could bear some relation with the density-driven structural changes in liquid water. Unfortunately, the two lines greatly differ from each other; in fact, their slopes even show opposite signs.

An inelastic x-ray scattering (IXS) study on liquid water under pressure, performed by some of the authors of this work, has investigated the density dependence of the high-frequency (terahertz) sound velocity, c_∞.[9] The c_∞ differs from the ultrasonic, adiabatic sound velocity c_s, because of the positive dispersion, a phenomenon that is ascribed to the presence of one or more relaxation processes and is found in all investigated liquids and glasses, along with dense supercritical fluids (see Refs. 10 and 11, and references therein). In fact, a relaxation process is characterized by a specific time scale τ, which marks the border between the "viscous liquidlike" dynamics [for $\omega_L(Q)\tau \ll 1$, where ω_L and Q are the sound frequency and wave vector, respectively] to the "elastic solidlike" one [$\omega_L(Q)\tau \gg 1$]. Correspondingly, the longitudinal sound velocity undergoes a transition (positive dispersion) from its "low" frequency, adiabatic limit, c_s, which characterizes the "liquid" value, to its "infinite" frequency limit $c_\infty > c_s$, characteristic of the "solid" response of the system. Liquid water, at room conditions, exhibits a very large positive dispersion; i.e., a large value of the ratio c_∞/c_s that is equal to 2.1, whereas this ratio is at the most 1.2 in simple liquids and simple, dense supercritical fluids (Refs. 10 and 11, and references therein). The relevant relaxation mechanism in liquid water is likely to be a structural relaxation process, related to the dynamics of making and breaking of the hydrogen bond network (Ref. 9, and references therein). The viscoelastic transition occurs, at room conditions, at $Q_t = 2$ nm^{-1} and acoustic energy $E = \hbar\omega_L(Q_t) = 3$ meV, which corresponds to a value of the acoustic frequency equal to 0.7 THz. Studies of the sound propagation in the terahertz regime can thereby provide a powerful probe of the dynamics of the hydrogen bond network on a mesoscopic (microscopic) length scale, whose outcome can be compared to the results of the structural studies. The IXS investigation of compressed water showed that the high-frequency sound velocity c_∞ increases with density much less than the adiabatic

sound velocity c_s.[9] In fact, the ratio c_∞/c_s decreases upon increasing density from 2.1, at room pressure, down to ~1.2 at 2.7 GPa, a value characteristic of simple liquids. Therefore, highly compressed water exhibits simple liquid dynamical features, which parallels the pressure-driven structural changes previously discussed. Furthermore, the IXS study revealed a remarkable cusp (~5% with respect to the smooth behavior) of c_∞ as a function of density, that seemed to indicate some anomalies in water at densities around 1.12 g/cm^3. It is important to note that the IXS study was not performed along an isothermal path. In fact, measurements were made along three different isothermal paths for different density ranges, at 277, 297, and 410 K, respectively. These were then merged together to obtain the extended density behavior of c_∞. Moreover, the experiment was performed using two different types of pressure cells and different instrumental energy resolutions. Water data utilizing the large-volume cell (sample volume 1 cm^3) were recorded with 1.6-meV energy resolution, while for the diamond anvil cell data (sample volume 10^{-5} cm^3) the energy resolution had to be relaxed to 3.0 meV in order to obtain a sufficient IXS signal.

In view of the nonisothermal character of the IXS study, the utilization of different pressure cells and instrumental configurations, and the controversial light-scattering results, we set out to perform an isothermal, high-pressure IXS study of c_∞, on a similar density range, in order to check for the existence of the cusp, an aspect that has important consequences for the properties of liquid water.

The experiment was carried out on beam line ID28 at the European Synchrotron Radiation Facility (ESRF), using the silicon (9 9 9) setup with a total energy resolution of 3.0 meV. The focal spot of the monochromatic (17 794 eV) x-ray beam had a full width at half maximum equal to 30 (horizontal) by 80 (vertical) μm^2. We utilized a diamond anvil cell (DAC) of the membrane type, equipped with 600-μm culet diamonds. Rhenium or stainless steel was used as the gasket material. The sample chamber dimensions were ~300 μm in diameter, and 80–100 μm in thickness. The cell was loaded by dropping high-purity water in the sample chamber. A ruby chip (5 μm diameter) for pressure measurements[12] was placed very close to the edge. Experimental errors on single pressure measurements were equal to ~±0.01 GPa. The DAC was placed into a vacuum chamber in order to minimize and control the empty cell contributions to the scattering signal.[13] A more detailed description of the beam-line setup and of the vacuum chamber can be found elsewhere.[10,13] The IXS measurements were performed at room temperature (295 K) between 0.05 and 0.88 GPa, and data points at each temperature were taken in the 3–13 nm^{-1} Q-transfer range at $\Delta Q = 1.2$ nm^{-1} intervals in order to extract a reliable dispersion relation.

Typical IXS spectra as a function of Q and pressure are reported in Fig. 1 for four selected Q and pressure values. All the spectra clearly show the elastic line, along with two inelastic peaks corresponding to the acoustic excitations. With increasing Q the inelastic peaks shift towards higher energies, showing the dispersion of sound propagation, and continuously broaden. At fixed Q, the acoustic excitation energy increases with pressure, testifying the increase of the sound

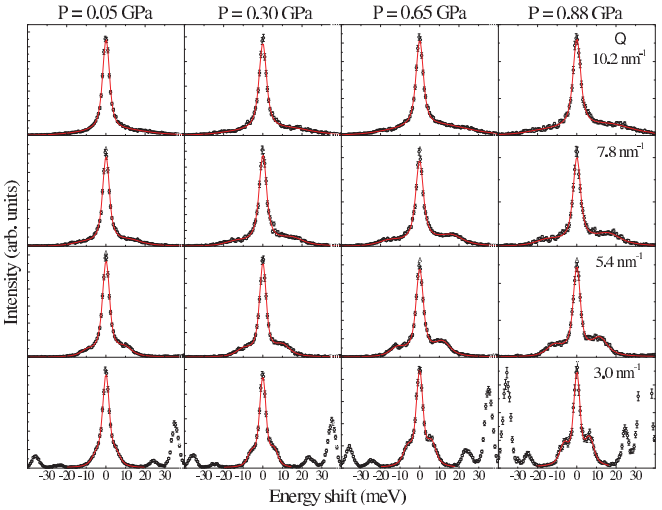

FIG. 1. (Color online) Selected IXS spectra of liquid water as a function of Q (columns) and pressure (rows), at room temperature (295 K). Data are compared to the model fit function [red (gray) lines] as explained in the text. The transverse and longitudinal acoustic phonons of diamond are visible above 20 meV, at 3.0 nm^{-1}.

velocity. The spectra were analyzed using a viscoelastic model, based on the memory function formalism, which describes the relaxation dynamics of the fluid in terms of different, empirical, relaxation time scales.[10,11] The model dynamic structure factor $S(Q,\omega)$, that is symmetric around $\omega = 0$, was first multiplied by the Bose quantum population factor, in order to properly reproduce the Stokes (anti-Stokes) detailed balance. The resulting function was then convoluted with the experimentally determined spectral resolution function and finally fitted to the IXS spectra utilizing a standard χ^2 minimization routine. The resulting fits are as well reported

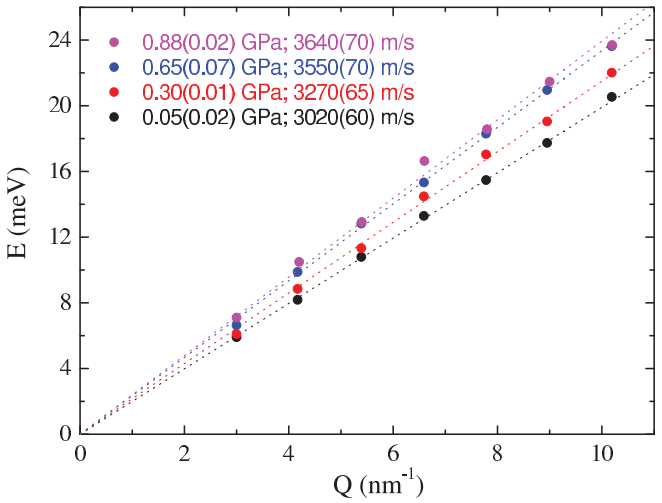

FIG. 2. (Color online) Acoustic excitation energy E as a function of momentum transfer Q at the four selected pressures already considered in Fig. 1. The dashed lines are linear fits to the data, and the resulting high-frequency sound velocities are reported in the inset. Errors on pressures include inaccuracy in the single pressure measurements and pressure changes which occurred during the IXS measurement. Errors on sound velocities are obtained from the linear fit to the data points.

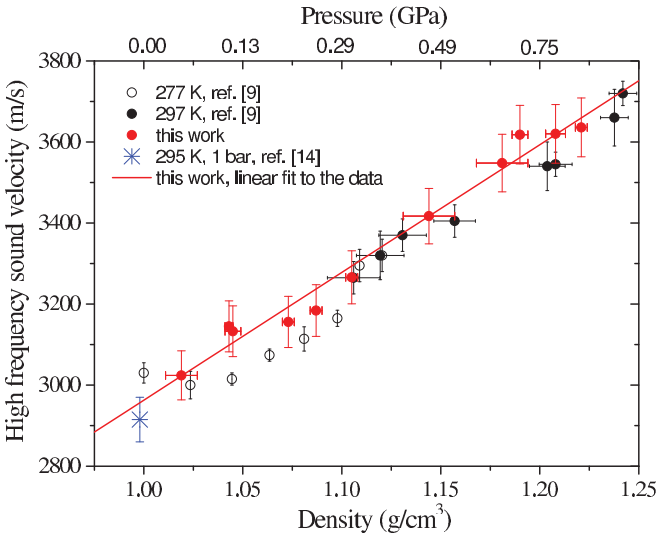

FIG. 3. (Color online) Density dependence of the high-frequency sound velocity c_∞ in liquid water. The corresponding nonlinear pressure scale at 297 K is reported on the upper horizontal scale. The equation of state is taken from the NIST database (Ref. 15). Red (gray) dots: data of this work 295 K; black, full (open) dots: data from Ref. 9, at 297 (277) K; asterisk: value at 1 bar and 295 K, obtained from data in Ref. 14. The continuous line is a linear fit to the data points of this work.

in Fig. 1. Once the fitted $S(Q,\omega)$ is obtained, the acoustic excitation energy $E(Q)$ is determined as $E(Q) = \hbar\omega_L(Q)$, where $\omega_L(Q)$, the apparent sound frequency, is the frequency of the maximum of the longitudinal current correlation function $J(Q,\omega) = (\omega/Q)^2 S(Q,\omega)$. In Fig. 2 we report $E(Q)$ at the four selected pressures already considered in Fig. 1. The Q behavior of the acoustic energies is quite linear in the investigated Q range, implying that the apparent sound velocity c_L, given by $c_L(Q) = \omega_L(Q)/Q$, is Q independent. As the sound propagation is definitely beyond the viscoelastic transition in our Q interval (see Ref. 9 and references therein), the sound propagates in the elastic, solidlike regime, which in turn allows us to identify c_∞ with c_L. In Fig. 3 we report the high-frequency sound velocity as a function of density; pressures at room temperature are reported on the upper, nonlinear horizontal scale. The density behavior of c_∞ is quite smooth and is well described by a linear law, closely resembling the Birch law for adiabatic sound propagation in dense materials. The linear behavior extrapolates well to the value of c_∞ at room conditions, reported in a different run of IXS measurements.[14] Also, previous data at room temperature[9] are consistent, within the error bars, with our density behavior of c_∞. On the other hand, the low-temperature (277 K) literature data[9] exhibit a different density behavior than observed here. Most importantly, the present density behavior of c_∞ definitely rules out the previously observed cusp at $\sim$1.12 g/cm^3.[9] We note that the cusp was based on the comparison of the density behavior of c_∞ along the two isothermal compression paths at 277 K and room temperature. Unfortunately, there is little overlap between the two density ranges, and the small overlap is also very close to the density value of the cusp. In addition, the values of c_∞ at the two temperatures, in the small overlapping density ranges, are consistent within the error bars, which in turn led the authors to conclude that c_∞ does not depend on the temperature, while it only depends on the density. The density behaviors of c_∞ measured at different temperatures were then merged together to obtain an extended density dependence of c_∞. Under this light, the cusp at 1.12 g/cm^3 is immediately evident. On the other hand, previous isochoric measurements of c_∞ at 1–2000 bar and 273–473 K show overall changes of this quantity of the order of 20%.[14] Consequently, it appears that merging data on c_∞ at different temperatures is definitely an incorrect procedure. Under this new light, the cusp is rather an artifact produced by what is likely to be the fortuitous cross of the two different density behaviors of c_∞ at 277 K and room temperature, which were improperly merged together.

In summary, we investigated the density behavior of the high-frequency sound velocity of water, in the terahertz regime, at room temperature, in the density (pressure) range of 1.02–1.22 g/cm^3 (0.05–0.88 GPa). A smooth, linear behavior was found, that rules out the previously observed anomaly (cusp)[9] obtained as a result of incorrectly merging nonisothermal data. We think our study can provide a useful constraint to the different theories on liquid water.

We acknowledge the ESRF for provision of beam time at ID28, and we thank D. Gambetti, M. Hoesch, J. Serrano-Gutierrez, A. Beraud, and A. Bossak for fruitful discussions and assistance during the experiments. Two of us, F.A.G. and M.S., have been supported by the European Community, under Contract No. FP7 G.A. No 228334 Laserlabeurope. T.S. has received funding from the European Research Council under the European Community's Seventh Framework Program (FP7/2007-2013)/ ERC grant Agreement No. 207916.

*santoro@lens.unifi.it

[1] A. K. Soper and M. A. Ricci, Phys. Rev. Lett. **84**, 2881 (2000).
[2] A. M. Saitta and F. Datchi, Phys. Rev. E **67**, 020201(R) (2003).
[3] Th. Strässle, A. M. Saitta, Y. Le Godec, G. Hamel, S. Klotz, J. S. Loveday, and R. J. Nelmes, Phys. Rev. Lett. **96**, 067801 (2006).
[4] G. Weck, J. Eggert, P. Loubeyre, N. Desbiens, E. Bourasseau, J. B. Maillet, M. Mezouar, and M. Hanfland, Phys. Rev. B **80**, 180202 (R) (2009).
[5] O. Mishima and H. E. Stanley, Nature **396**, 329 (1998).
[6] L. Xu, P. Kumar, S. V. Buldyrev, S. H. Chen, P. H. Pool, F. Sciortino, and H. E. Stanley, Proc. Natl. Acad. Sci. USA **102**, 16558 (2005).
[7] F. Li, Q. Cui, Z. He, T. Cui, J. Zhang, Q. Zhou, G. Zou, and S. Sasaki, J. Chem. Phys. **123**, 174511 (2005).
[8] T. Kawamoto, S. Ochiai, and H. Kagi, J. Chem. Phys. **120**, 5867 (2004).

[9]M. Krisch, P. Loubeyre, G. Ruocco, F. Sette, A. Cunsolo, M. D'Astuto, R. LeToullec, M. Lorenzen, A. Mermet, G. Monaco, and R. Verbeni, Phys. Rev. Lett. **89**, 125502 (2002).
[10]F. A. Gorelli, M. Santoro, T. Scopigno, M. Krisch, and G. Ruocco, Phys. Rev. Lett. **97**, 245702 (2006).
[11]G. G. Simeoni, T. Bryk, F. Gorelli, M. Krisch, G. Ruocco, M. Santoro, and T. Scopigno, Nat. Phys. **6**, 503 (2010).
[12]H. K. Mao, J. Xu, and P. M. Bell, J. Geophys. Res. **91**, 4673 (1986).
[13]F. A. Gorelli, M. Santoro, T. Scopigno, M. Krisch, T. Bryk, G. Ruocco, and R. Ballerini, Appl. Phys. Lett. **94**, 074102 (2009).
[14]G. Monaco, A. Cunsolo, G. Ruocco, and F. Sette, Phys. Rev. E **60**, 5505 (1999).
[15]NIST Chemistry WebBook [http://webbook.nist.gov/chemistry/].